

Ablation of Intercepted Snow: Insights from In-Situ Observations in the Canadian Rockies

Authors:

Alex C. Cebulski¹ (ORCID ID - 0000-0001-7910-5056)

John W. Pomeroy¹ (ORCID ID - 0000-0002-4782-7457)

¹Centre for Hydrology, University of Saskatchewan, Canmore, Canada

Corresponding Author: Alex C. Cebulski, alex.cebulski@usask.ca

Key Points:

- New insights on the processes driving canopy snow ablation are presented based on in-situ observations and simulations from a novel process-based hydrological model.
- Canopy snow unloading was observed to be strongly associated with canopy snow load, wind speed and canopy snowmelt.
- Implementation of a revised canopy snow energy balance and unloading routine resulted in enhanced prediction of canopy snow ablation particularly for warm events compared to conventional approaches.

Abstract

Existing canopy snow ablation parameterizations have been shown to have uncertain transferability across differing climate and forest types. Moreover, many of the theories underlying the existing parameterizations have not been tested extensively across climate and forest

types. Here, novel snow interception process understanding, developed from fine-scale and high-frequency observations collected from needleleaf forests in the Canadian Rockies, is used to decouple the processes that initially load snow in the canopy from those that ablate it. A revised snow interception parameterization that calculates throughfall as a function of forest structure, is presented with modified canopy snow ablation parameterizations, and implemented in the Cold Regions Hydrological Modelling platform to simulate canopy snow load and subcanopy snowpack dynamics. To assess the effectiveness of these new parameterizations, simulations using both new and traditional routines were evaluated against observations of subcanopy snow water equivalent and canopy snow load at sites not used in model development, including the continental climate Marmot Creek, Alberta; subarctic climate Wolf Creek, Yukon Territory; and coastal climate Russell Creek, British Columbia (all in Canada). Preliminary results show that the revised interception parameterization improves predictability, increasing the R² compared to measurements from 0.4 with existing methods to 0.7 with the revised routine. This improved process understanding of snow interception and canopy snow ablation processes may have broad applicability and reliability, improving water resource assessment of forested, snow-dominated basins.

Thesis outline:

Previous studies have developed parameterizations to represent ablation processes including unloading, melt, drip and sublimation of snow intercepted in the canopy. However, these parameterizations have been shown to have uncertain transferability to new environments and have not yet been tested in discontinuous forest canopies. This study presents new in-situ measurements of canopy snow ablation processes and contrasts these observations with existing theories and models. Analysis of the canopy snow mass balance showed that unloading, drip and melt contributed to 60% of canopy snow ablation on average over two years with the remainder being attributed to canopy snow sublimation. The probability of unloading, drip and melt was observed to increase with air temperature and wind speed. However, the probability of wind induced unloading was observed to decrease at warmer air temperatures. The probability of unloading due to warming was also observed to decline when wind speeds

were above 1 m s⁻¹. The increase in cohesion and adhesion of snow in the canopy at warmer temperatures and cooling due to wind-induced evaporation may contribute to the interaction multivariate interaction between air temperature, wind speed and canopy snow unloading. Exponential relationships were observed between both air temperature and wind speed with unloading and drip, which were also dependent on the amount of snow intercepted in the canopy. In comparison to existing models, this discontinuous forest exhibited unloading and drip due to warming at lower air temperatures. Conversely, wind-induced unloading occurred at higher wind speeds than predicted by current models.

1 Introduction

Accurate models of the seasonal subcanopy snowpack rely on a comprehensive understanding of snow interception and canopy snow ablation processes. The time that snow resides in the canopy, and is subjected to high rates of sublimation, is dependent on rates of canopy snow ablation processes. Existing theories on the initial loading of snow in the canopy are highly divergent and of uncertain application to differing environments, partly due to their varying inclusion of processes that ablate snow from the canopy.

The objective of this study is to determine if the theoretical underpinnings and assumptions behind existing canopy snow ablation parameterisations are supported by in-situ observations collected from a subalpine forest in the Canadian Rockies. This study specifically looks at canopy snow ablation after snowfall, initial interception has been discussed in Cebulski & Pomeroy (2025b).

Research Questions:

1. How does air temperature, wind, canopy snow sublimation and snowmelt influence the rate of snow unloading?
2. To what extent do current theoretical models of canopy snow ablation align with in-situ observations?

3. What modifications of existing models, if any, are necessary to accurately represent ablation of snow intercepted in the canopy and what is the performance of the updated model?

2 Study Site and Instrumentation

The observations presented in this study were collected at Fortress Mountain Research Basin (FMRB), AB, -115° W, 51° N, a continental headwater basin in the Canadian Rockies at 2100 m above sea level. Air temperature, humidity, and wind speed were measured at a height of 4.3 m at Forest Tower (FT) Station (Fig. 1). The precipitation rate was measured by an Alter-shielded OTT Pluvio weighing precipitation gauge installed 2.6 m above ground at Powerline Station. Incoming and outgoing solar radiation was measured by a Kipp & Zonen CNR4 4-Component Net Radiometer installed 3.27 m above the ground at Fortress Ridge Station. Three subcanopy lysimeters, consisting of a plastic horse-watering trough with an opening of 0.9 m² and depth of 20 cm suspended from a load cell, were installed to measure canopy snow unloading. A weighed tree lysimeter (subalpine fir) suspended from a load cell (Artech S-Type 20210-100) measured the weight of canopy snow load (kg) and was scaled to an areal estimate of snow load (mm) using snow surveys as in Pomeroy & Schmidt (1993). Additional details on this study site and the meteorological and lysimeter measurements have been described in Cebulski & Pomeroy (2025a). Four tipping bucket rain gauges, 3 Texas Electronics TR-525M and 1 Hyquest Solutions TB4MM were installed along a 15 m transect adjacent to the dense canopy subcanopy lysimeter to measure canopy snowmelt drainage. To isolate the subcanopy lysimeter measurements of canopy snow unloading from throughfall, 15-min intervals were selected that met the following criteria: no atmospheric precipitation, and snow was observed to be intercepted in the canopy using the weighed tree and timelapse imagery investigation.

A CSAT measured shear stress ... however it was frequently covered with snow during the ablation periods. So to provide a complete record of shear stress, a relationship between wind speed

at 4.3 m at FT station and shear stress from the CSAT (see supporting information). Shear stress was then gap filled when the CSAT was covered with snow using this relationship.

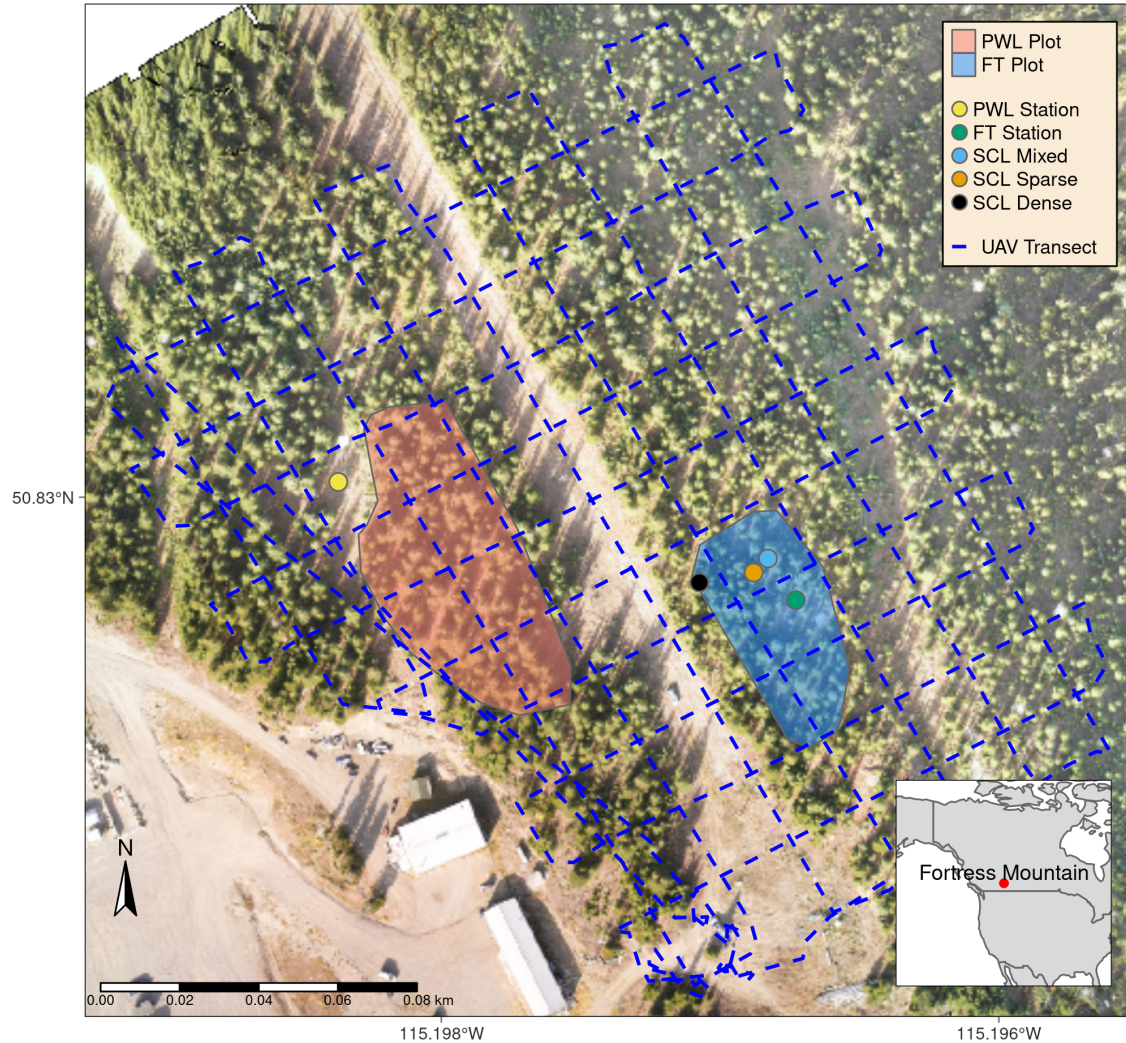


Figure 1: Map showing the location of forest plots, flux towers, subcanopy lysimeter instruments, and survey transects. The inset map on the lower right shows the regional location of Fortress Mountain Research basin.

3 Methods

3.1 Statistics on Canopy Snow Unloading Relationships

3.1.1 Combined influence of predictors on unloading

The influence of air temperature, wind speed, snow load, melt, and sublimation on the unloading process was assessed using a multivariate ordinary least squares (OLS) regression. The analyses tested the following hypotheses:

- a. Melt promotes unloading through loss of structural integrity, particle bond weakening, and lubrication.
- b. Sublimation promotes unloading via structural degradation and bond weakening.
- c. Wind promotes unloading through shear stress on snow, wind erosion, and branch movement.
- d. Air temperature promotes unloading by increased elasticity branches and association with melt/sublimation.

Because many of these processes occur simultaneously and could not be isolated experimentally, different combinations of the independent variables were included in the regression to identify which sets of processes significantly influenced unloading. The subcanopy lysimeter unloading measurements had a high relative instrument error due to the relatively small accumulation of unloaded snow over the 15-min intervals. To improve instrument accuracy, while maintain consistency of the unloading measurements with wind speed, the 15-min interval measurements of unloading were aggregated over differing predictor variable bins. Air temperature and wind speed were measured at FT station, canopy snow load from the weighed tree lysimeter (scaled to the canopy of each respective subcanopy lysimeter), and canopy snowmelt and sublimation simulated in CRHM. Sublimation was simulated using Equation 10 following Essery et al. (2003) and snowmelt calculated using available energy from Equation 3 both implemented in CRHM, were used for this analysis. Bins that had accumulated unloaded snow less than 0.1

mm were removed which resulted in a mean instrument error of +/- 2% for the remaining bins. The individual processes found to be significant predictors of unloading in the multivariate regression (i.e., shear stress and canopy snow melt) were then isolated to parameterise a model of their effects.

3.1.2 Wind induced unloading

The influence of wind, shear stress and canopy snow load on unloading was assessed during intervals without canopy snowmelt. These periods were defined using simulated canopy snowmelt in CRHM and by visual analysis of time-lapse imagery. By excluding periods influenced by melt, the snow captured by the lysimeters is attributed primarily to wind-driven unloading. Although unloading resulting from snow metamorphism or thermally induced branch bending may also contribute, the observed unloading is interpreted to be predominantly wind-induced over these intervals. The relationship between wind speed, shear stress, canopy snow load, and unloading was analyzed using linear and non-linear least squares regression, with shear stress modeled linearly and wind speed modeled exponentially.

3.1.3 Canopy snowmelt induced unloading

A mass balance approach was incorporated to determine the unloading rate resulting from canopy snowmelt (q_{unld}^{melt} , mm s⁻¹). The influence of canopy snowmelt on q_{unld}^{melt} was then assessed by fitting a linear model using an ordinary least squares regression. Since direct measurements of canopy snow unloading are challenging to obtain independently from canopy snowmelt drainage (Storck et al., 2002), the following mass balance was incorporated to determine q_{unld}^{melt} as a residual:

$$\frac{dL}{dt} = [q_{sf} - q_{tf} + q_{ros}] - [q_{unld}^{melt} + q_{unld}^{wind}] - q_{drip} - q_{wind}^{veg} - q_{sub}^{veg} \quad (1)$$

where $\frac{dL}{dt}$ is the change in canopy snow load over time, (mm s^{-1}), q_{sf} is the snowfall rate (mm s^{-1}), q_{tf} (mm s^{-1}) is the throughfall rate (mm s^{-1}), q_{ros} (mm s^{-1}) is the rate of rainfall falling on snow intercepted in the canopy, q_{unld}^{melt} is the canopy snow unloading rate due to melt (mm s^{-1}), q_{unld}^{wind} is the canopy snow unloading rate due to wind (mm s^{-1}), q_{drip} is the canopy snow drip rate resulting from canopy snowmelt (mm s^{-1}), q_{wind}^{veg} is the wind transport rate in or out of the control volume (mm s^{-1}), and q_{sub}^{veg} is the intercepted snow sublimation rate (mm s^{-1}). Figure 1 in Cebulski & Pomeroy (2025b) presents a visual representation of this mass balance. Little research has examined the water-holding capacity of snow intercepted in the canopy; however in this study it is assumed to be minimal such that $q_{drip} \approx q_{melt}$.

Then Equation 1 was rearranged to solve for q_{unld}^{melt} during intervals without $[q_{sf} - q_{tf} + q_{ros}]$ or q_{wind}^{veg} as:

$$q_{unld}^{melt} = -\frac{dL}{dt} - q_{drip} - q_{unld}^{wind} - q_{sub}^{veg} \quad (2)$$

While some components of the canopy snow mass balance can be measured directly with relative ease, such as $\frac{\Delta L}{\Delta t}$ with the weighed tree, sublimation of canopy snow is more difficult to quantify directly especially in forested mountain environments (Conway et al., 2018; Helgason & Pomeroy, 2012b) and thus q_{sub}^{veg} was simulated in this study in CRHM using Equation 10 as described in Essery et al. (2003). q_{drip} was measured where possible using the tipping buckets, however problems with freezing of liquid water in the devices limited the amount of q_{drip} that could be collected. Thus, q_{drip} was also supplemented with simulated canopy snowmelt (q_{melt}) in CRHM as in Equation 3. Canopy snow ablation periods that were dominated by melt were selected for calculating q_{unld}^{melt} where the contribution of q_{unld}^{wind} and q_{sub}^{veg} to canopy snow ablation was less than 5%.

4 Canopy Snow Energy Balance

A revised canopy snow energy balance is presented here which provided both an approximation of canopy snowmelt and sublimation as these processes could not be measured directly and also for use in the canopy snow ablation routines. The energy available for melting snow intercepted in the canopy, Q_{melt} (W m^{-2}), which is a function of the canopy snow load (L) was calculated as:

$$Q_{melt}(L) = Q_{sw} + Q_{lw} + Q_p + Q_h + Q_l - [C_p^{ice} L \frac{\Delta T_{vs}}{\Delta t}] \quad (3)$$

where Q_{sw} and Q_{lw} (W m^{-2}) are the net shortwave and longwave radiation heat fluxes to the canopy snow, Q_p (W m^{-2}), is the advective energy rate, and Q_l and Q_h (W m^{-2}), are the turbulent fluxes of latent heat and sensible heat respectively (positive towards canopy snow), C_p^{ice} ($\text{J kg}^{-1} \text{ K}^{-1}$) is the specific heat capacity of ice, and $\frac{\Delta T_{vs}}{\Delta t}$ (K s^{-1}) is the change in canopy snow temperature over time.

Q_{sw} was determined as:

$$Q_{sw} = \downarrow Q_{sw} \cdot (1 - \alpha_s) \cdot \tau_{50}^{veg} \quad (4)$$

where $\downarrow Q_{sw}$ is the downwelling shortwave radiation (W m^{-2}), α_s is the albedo of snow intercepted in the canopy (-), τ_{50}^{veg} (-) is the canopy transmittance to $\downarrow Q_{sw}$. τ_{50}^{veg} was determined using Equation from Pomeroy et al. (2009) with half of the leaf area index (LAI), following studies (Kesselring et al., 2024; Weiskittel et al., 2009), who report that approximately 50% of the total leaf area is concentrated in the upper half of coniferous canopies. This provides an approximation of the mean Q_{sw} to all snow intercepted in the canopy, and is a simplification from using a partial differential equation to determine the radiation incident to individual height layers within the canopy. Upwelling shortwave radiation reflected off of the surface

snowpack is considered negligible contribution to the snow intercepted in the canopy as it is primarily blocked by vegetation elements underlying the canopy snow.

Q_{lw} was approximated as:

$$Q_{lw} = \downarrow Q_{lw}^{atm} + \uparrow Q_{lw}^{veg} + \uparrow Q_{lw}^{veg2veg} - Q_{lw}^{vs} \quad (5)$$

where Q_{lw}^{atm} is the downwelling longwave radiation from the atmosphere (W m^{-2}), Q_{lw}^{veg} is the longwave radiation upwelling from vegetation elements underlying snow intercepted in the canopy (W m^{-2}), $Q_{lw}^{veg2veg}$ is the downwelling longwave radiation emitted from the underside of the vegetation elements reflected by the subcanopy snowpack (W m^{-2}), and Q_{lw}^{vs} (W m^{-2}) is the outgoing longwave radiation from the top and bottom of the canopy snow layer calculated as:

$$Q_{lw}^{vs} = 2\epsilon_s \sigma T_{vs}^4 \quad (6)$$

where ϵ_s is the emissivity (-) of snow taken as 0.99 and σ is the Stefan–Boltzmann ($5.67e-10 \text{ W m}^{-2} \text{ K}^{-4}$). Q_{lw}^{atm} was approximated in this study as in Sicart et al. (2006) to take into account the influence of atmospheric moisture on emissivity. Q_{lw}^{veg} was calculated with the assumption that canopy elements were in equilibrium with the air temperature plus any change in vegetation temperature from the extinction of $\downarrow Q_{sw}$ in the canopy (Pomeroy et al., 2009, Eq. 4).

Q_p was calculated as:

$$Q_p = [C_p^{wtr} m_r (T_r - T_{vs}) + C_p^{ice} m_s (T_s - T_{vs})] / \Delta t \quad (7)$$

where C_p^{wtr} is the specific heat capacity of water ($\text{J kg}^{-1} \text{ K}^{-1}$), m_r is the specific mass of liquid water in precipitation (mm), T_r is the rainfall temperature (K), m_s is the specific mass of snow

in precipitation (mm), and T_s is the snowfall temperature (K).

Q_h was calculated as:

$$Q_h = \frac{\rho_a}{r_a} C_p^{air} (T_a - T_{vs}) \quad (8)$$

where ρ_a is the air density (kg m^{-3}), C_p^{air} is the specific heat capacity of air ($\text{J kg}^{-1} \text{ K}^{-1}$), T_a is the air temperature, and r_a is the aerodynamic resistance (s m^{-1}) which was approximated from Equation 4 from Allan et al. (1998) as:

$$r_a = \frac{\log(\frac{z_T-d_0}{z_0})\log(\frac{z_u-d_0}{z_0})}{\kappa^2 u_z} \quad (9)$$

where z_T is the height of temperature measurement (m), d_0 is the displacement height (m) which was approximated as $2/3^{\text{rd}}$ the mean canopy height, z_0 is the roughness length (m) which was approximated as $1/10^{\text{th}}$ of the mean canopy height, z_u is the wind speed measurement height (m), κ is von Karman's constant, 0.41 (-), and u_z is the wind speed measurement at z_u (m s^{-1}).

Q_l was calculated as:

$$Q_l = \frac{\rho_a}{r_i + r_a} (q_a(T_a) - q_{vs}(T_{vs})) \quad (10)$$

where r_i is a resistance for transport of moisture from intercepted snow to the canopy air space (Eq. 28 in Essery et al., 2003), $q_a(T_a)$ and $q_{vs}(T_{vs})$ are the specific humidity (-) at the air temperature and canopy snow temperature respectively. If the height of the air temperature measurement differs from the humidity measurement the z_T term in the Equation 9 should be adjusted to use the the humidity measurement height.

The above sensible and latent heat flux equations assume neutral atmospheric stability conditions, i.e., nearly adiabatic conditions (no heat exchange) which may be appropriate for

application with snow which is intercepted in the roughness elements where stability corrections may not be required (Allan et al., 1998). This is also supported by the uncertainty of stability correction in forest canopies (Conway et al., 2018) and mountain environments (Helgason & Pomeroy, 2012a). Solving Equation 3 requires an iterative solution to determine ΔT_{vs} and the remaining terms which are also a function of T_{vs} .

5 Modelled Canopy Snow Energy and Mass Balance

The energy and mass balance of canopy snow was simulated using the Cold Regions Hydrological Model (CRHM) to evaluate the new canopy snow ablation routine. A full description of the CRHM model is described in Pomeroy et al. (2007) and the up to date source code is available at <https://github.com/srlabUsask/crhmcodes>. In addition to the updated parameterizations presented in this study, parameterizations from previous studies that simulate canopy snow unloading, melt, and sublimation were also implemented and compared against the updated routine within CRHM. Canopy snow sublimation simulations also provided the rate of sublimation needed in Equation 2.

In addition to the updated parameterizations presented in this study, three other canopy snow routines were implemented in CRHM following previous studies by Ellis et al. (2010) and Floyd (2012) (hereafter Ellis2010), Roesch et al. (2001) (Roesch2001), and Andreadis et al. (2009) (Andreadis2009). The Ellis et al. (2010) routine was previously integrated into CRHM as a module and is the one typically used to simulated snow accumulation in forests in CRHM and was run as is. The Ellis2010 module includes canopy snow sublimation as described in Pomeroy et al. (1998), canopy snow unloading over time from Hedstrom & Pomeroy (1998) with modifications described in Floyd (2012) to handle canopy snow melt and drip processes using an ice-bulb temperature threshold. The Roesch2001 routine represents canopy snow unloading and melt using wind and air temperature functions. The Andreadis2009 parameterization unloads snow as a function of canopy snowmelt alone, following observations by Storck et al. (2002) and does not include wind induced unloading. The snowmelt rate from

Equation 3 was used to calculate the unloading rate for the Andreadis2009 unloading. The default parameters provided by each individual study were used here and were not calibrated. More details on the aforementioned parameterizations are described in Cebulski & Pomeroy (2025b).

6 Results

6.1 Canopy Snow Unloading Relationships

A positive relationship ($p < 0.05$, $R^2 = 0.79$) was identified between canopy load, canopy snowmelt, wind speed, and the rate of canopy snow unloading, as measured by the subcanopy lysimeters. This set of predictors yielded the highest R^2 among the models tested (Table 1). Shear stress was found to explain less variability compared to wind speed, when combined with canopy snow load and snowmelt ($p < 0.05$, $R^2 = 0.71$). Air temperature and canopy snow sublimation were not significant predictors in any model ($p > 0.05$; Table 1). A model including only canopy load, air temperature, and wind speed produced an R^2 of 0.11, though only canopy load and wind speed were statistically significant ($p < 0.05$). As shown in Fig. 2, unloading rates were substantially more variable across the canopy snowmelt and sublimation bins ($0\text{--}2 \text{ mm hr}^{-1}$) compared to the air temperature and wind speed bins ($0\text{--}0.5 \text{ mm hr}^{-1}$). As a result, models without canopy snowmelt explained substantially less variation in unloading. Additional model comparisons with various combinations of independent variables are presented in the supporting information.

The mean unloading rate was observed in Fig. 2 to increase with increasing canopy load, air temperature, ice-bulb temperature depression, shear stress, and wind speed. Despite the insignificant relationships, air temperature and canopy snow sublimation were positively associated with canopy snow unloading, though for sublimation this relationship was limited to sublimation rates between 0 and 0.3 mm hr^{-1} (Fig. 2). For sublimation rates higher than 0.3 hr^{-1} , unloading is observed to decline with increasing sublimation, as more canopy snow is

partitioned to the atmosphere. A decline in unloading is observed for wind speed bins above 3 m s⁻¹ which is attributed to some wind transport of canopy snow, and potential entrainment into the atmosphere, and corresponding increased sublimation rates.

Table 1: Summary of multiple linear regression results evaluating all combinations of predictor variables for canopy snow unloading including: canopy load (L), wind speed (u), canopy snowmelt rate (q_{melt}), canopy snow sublimation rate (q_{subl}), and air temperature (T_a). Columns L to Ta show the coefficient estimate for each respective term, and the significance of each term is shown in brackets. Significance codes: * = p < 0.05; ns = not significant (p > 0.05). The models are ranked by their corresponding AIC value.

Model									
Name	Intercept	L	u	q_{melt}	q_{subl}	τ	T_a	R^2	AIC
M1	-0.11 (ns)	0.02 (*)	0.08 (*)	0.40 (*)	—	—	—	0.79	- 12.8
M4	-0.08 (ns)	0.04 (*)	—	0.39 (*)	—	0.75	—	0.71	5.5
M7	0.13 (ns)	0.02 (*)	—	0.32 (*)	-0.22	—	—	0.54	10.0
M10	-0.06 (ns)	0.02 (*)	0.08 (*)	0.38 (*)	—	—	0.00	0.52	-4.4
M24	-0.00 (ns)	0.02 (*)	0.05 (*)	0.36 (*)	0.13	—	—	0.37	-2.0
M40	0.07 (ns)	0.01 (*)	0.06 (*)	—	—	—	0.01	0.11	2.4
M63	0.22 (*) (ns)	0.00 (ns)	-0.01 (ns)	—	0.07 (ns)	—	—	- 0.02	39.8

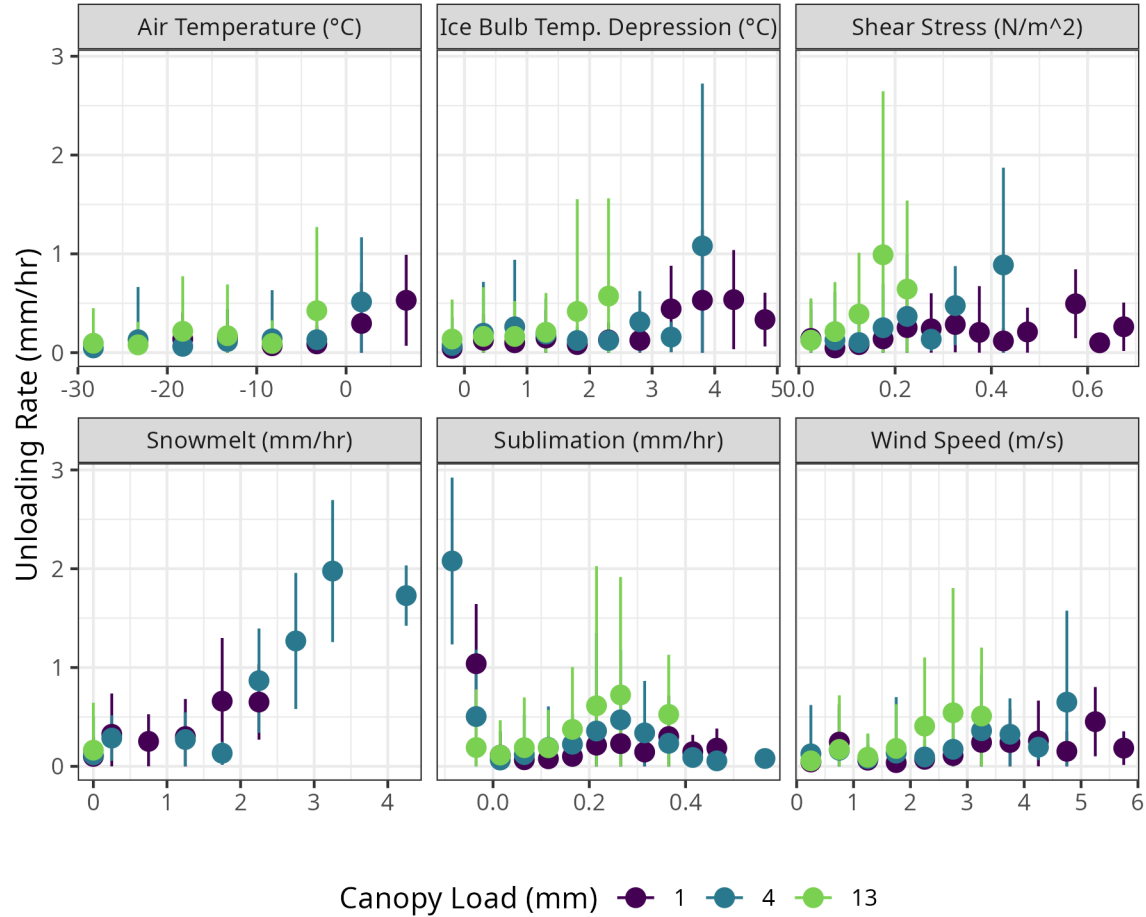


Figure 2: Scatter plots showing the mean canopy snow unloading rate for differing bins of air temperature ($^{\circ}\text{C}$), ice-bulb temperature depression ($^{\circ}\text{C}$), shear stress (N m^{-2}), canopy snowmelt (mm hr^{-1}), canopy snow sublimation (mm hr^{-1}), and wind speed (m s^{-1}). Note: canopy snow unloading was measured by the subcanopy lysimeters, air temperature and wind speed were measured at FT station, canopy snowmelt and sublimation were modelled in CRHM.

6.1.1 Wind Induced Unloading

Canopy snow unloading measurements from the subcanopy lysimeters, filtered to include intervals without canopy snowmelt, followed a positive linear relationship with shear stress and a positive exponential relationship with wind speed (Fig. 3). Based on these observed relation-

ships the following relationships were fit and tested against the observed data:

The wind-driven canopy snow unloading rate, q_{unld}^{wind} , was represented as a linear function of shear stress:

$$q_{unld}^{wind} = L \cdot \tau_{mid} \cdot a \quad (11)$$

where τ_{mid} is the shear stress at mid canopy height and a is a fitting constant.

An exponential function of wind speed was defined as:

$$q_{unld}^{wind} = L \cdot u_{mid} \cdot a \cdot e^{b \cdot u_{mid}} \quad (12)$$

where u_{mid} is the wind speed at mid canopy height, and a and b are fitting constants.

The shear stress relationship (Equation 11) accounted for slightly more variability in unloading ($p < 0.05$, $R^2 = 0.61$), likely due to its better relation to the kinetic energy required to unload snow compared to wind speed ($p < 0.05$, $R^2 = 0.54$). The mean bias of the shear stress model of 0.037 mm hr^{-1} is also lower compared to the wind speed model of 0.048 mm hr^{-1} , additional model error statistics and fitting coefficients are provided in Table 2. Both models exhibited considerable scatter across the different bins, with notable uncertainty within each bin (Fig. 3). The wind-induced unloading rate was observed to be higher for bins with higher canopy snow load across nearly all bins (Fig. 3). The R^2 of both the shear stress and wind speed relationships is much higher than the amount of variance explained by wind speed when including intervals with melting snow (Table 1). The increased liquid water content during the canopy snowmelt process may provide some resistance to wind induced unloading. However, a statistically significant negative influence of air temperature on wind speed could not be found, likely due to the strong positive association of air temperature and melt on unloading. Moreover, increased canopy snow unloading during low wind speeds, resulting from high melt rates could also contribute to the lower explanatory power of wind speed in

Table 1. The higher R^2 of the shear stress model compared to wind speed, coupled with the better physical representation of kinetic energy, provided the reasoning for selecting shear stress as the independent variable to predict wind-induced unloading.

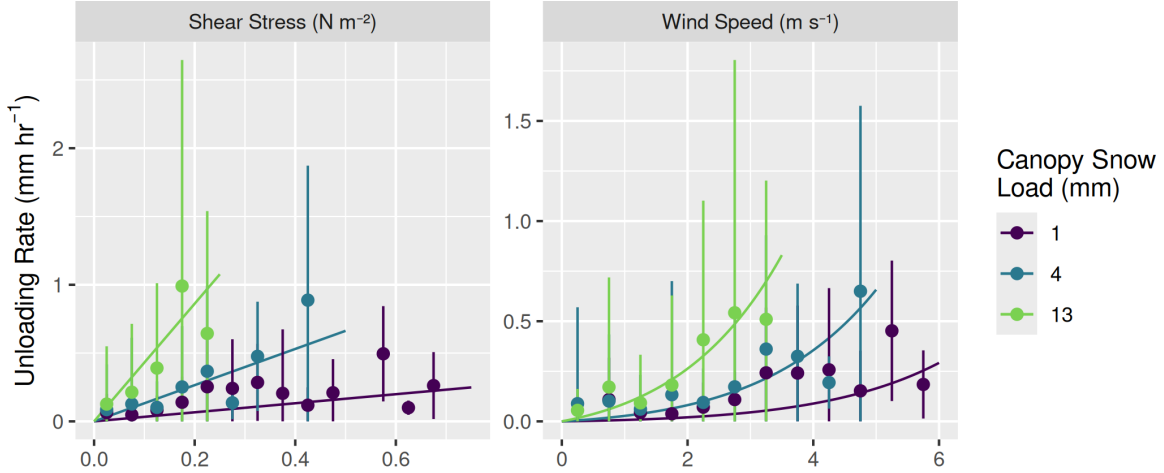


Figure 3: Canopy snow unloading rate measured by the subcanopy lysimeters versus shear stress (left) and wind speed (right) during periods without canopy snowmelt. The dots represent mean unloading rates within bins of shear stress and wind speed; error bars indicate ± 1 standard deviation. The fitted lines show predictions from Equation 11 (left) and Equation 12 (right).

Table 2: Summary of the performance and regression coefficients for the relationship between canopy snow unloading with wind speed (Equation 11) and shear stress (Equation 12), as shown in Fig. 3. Coefficients are developed for hourly unloading.

Metric	Wind	Shear Stress
Mean Bias (mm/hr)	0.048	0.037
Mean Absolute Error (mm/hr)	0.087	0.115
Root Mean Square Error (mm/hr)	0.11	0.15
Coefficient of Determination (R^2)	0.54	0.61
Coefficient a	4.62e-03	3.31e-01
Significance of a	p < 0.05	p < 0.05

Table 2: Summary of the performance and regression coefficients for the relationship between canopy snow unloading with wind speed (Equation 11) and shear stress (Equation 12), as shown in Fig. 3. Coefficients are developed for hourly unloading.

Metric	Wind	Shear Stress
Coefficient b	3.93e-01	NA
Significance of b	p < 0.05	NA

6.1.2 Melt induced unloading

A positive linear relationship was identified between the ratio of canopy snow unloading to melt and canopy snow load (Fig. 4). This ratio ranged from approximately 0–0.5 for snow loads between 0 and 5 mm, and increased to a maximum of 5 at a canopy snow load of 30 mm (Fig. 4). This relationship was represented by the following equation:

$$q_{unld}^{melt} = f(m) \cdot q_{melt}(L) \quad (13)$$

where $f(m)$ is the ratio of unloading to canopy snowmelt and q_{melt} is the canopy snowmelt rate (mm hr^{-1}). Equation 13 is similar to Equation 33 in Andreadis et al. (2009); however, instead of assuming a constant value of 0.4 for $f(m)$, it was determined as:

$$f(m) = m \cdot L + b \quad (14)$$

where m and b were determined as 0.16 and -0.5, respectively, using an ordinary least squares regression.

Equation 13 resulted in a statistically significant relationship ($p < 0.05$, $R^2 = 0.73$) for canopy snow ablation events in which wind-driven unloading and/or sublimation contributed less than 5% to total ablation less than 5%, based on ordinary least squares linear regression (Fig. 4).

The regression was performed using the data shown in Fig. 4, which presents the ratio of canopy snow unloading, derived from the weighed tree using Equation 2 using simulated q_{melt} . Additional observations of canopy snowmelt melt from the tipping buckets were also used to compute the canopy snow unloading-to-melt ratio (Fig. 4); however, the number of usable observations was limited due to freeze-thaw events that affected the instrument functionality. These measurements are still useful in providing some indication of the validity of the CRHM canopy snowmelt/drip routine (Fig. 8). The CRHM estimated cumulative drip is higher than the tipping buckets for two out of the three melt events. A difference in the timing and magnitude of the observed and simulated values were expected due to both instrument uncertainties in the tipping buckets (freezing/thawing) and in the canopy snow energy balance simulation.

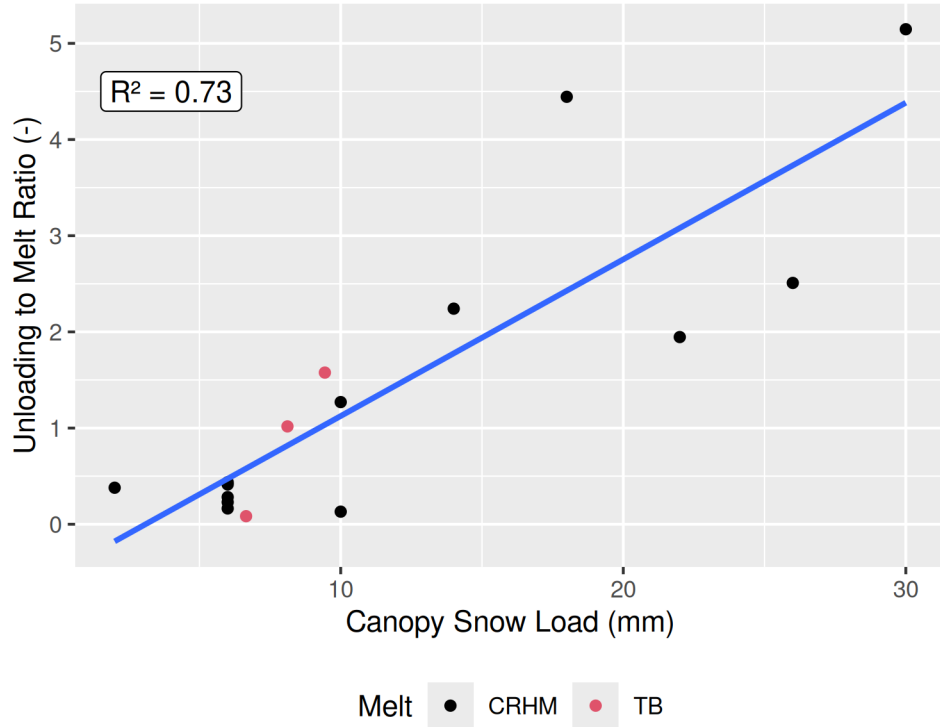


Figure 4: The ratio of canopy snow unloading (weighed tree residual) to snowmelt across different canopy snow load bins and events. Black dots represent the observed cumulative unloading divided by the cumulative simulated snowmelt from CRHM. Red dots show the cumulative observed unloading divided by snowmelt measured by the tipping buckets. Multiple dots within a bin correspond to different events. The blue line represents the best-fit line derived from ordinary least squares regression.

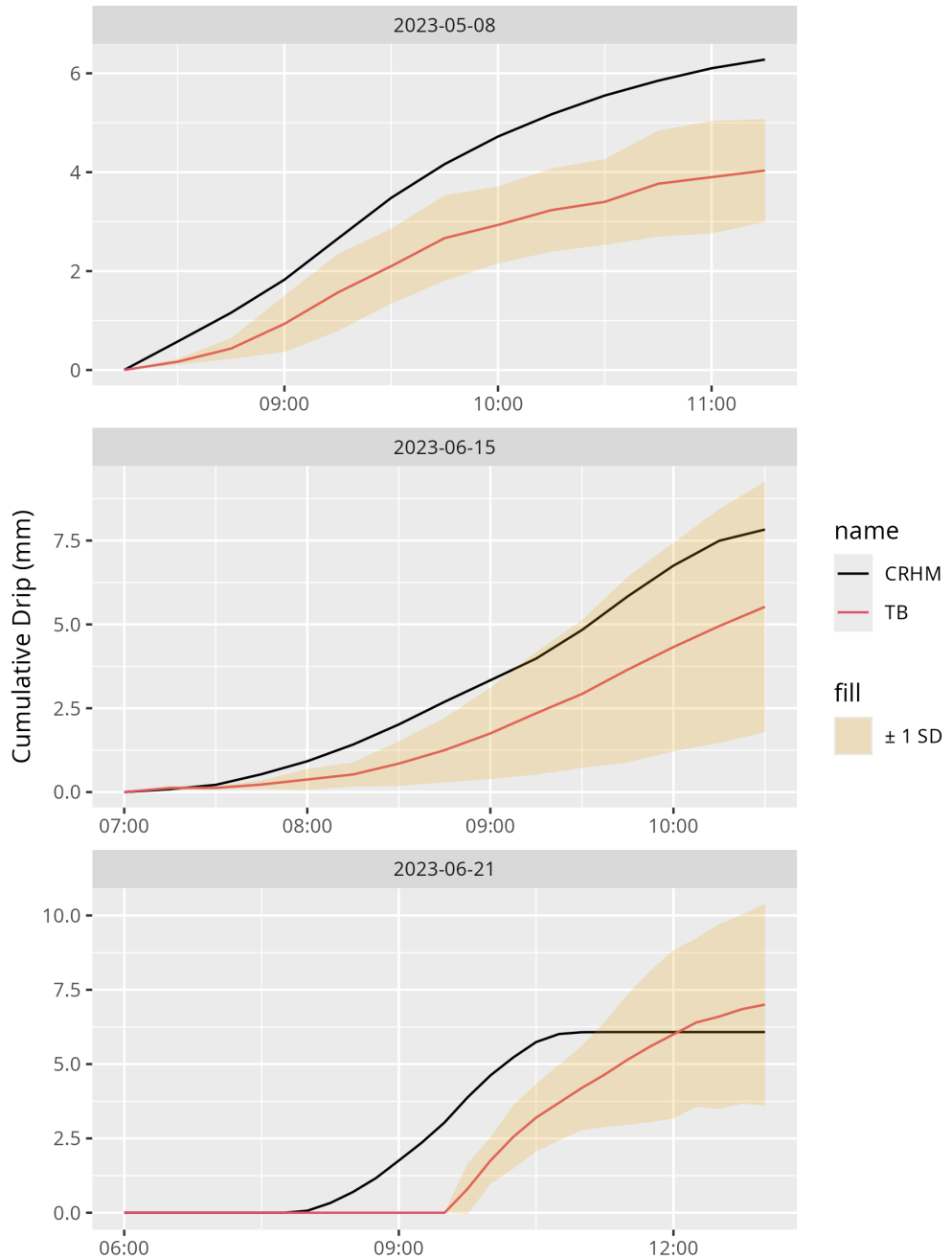


Figure 5: Cumulative canopy snow drip from the mean of the tipping buckets (TB_mean) and the updated canopy snowmelt routine (crhm_drip).

6.2 Evaluation of canopy snow ablation parameterisations

The updated canopy snow ablation routine which includes canopy snowmelt estimated from the energy balance described by Equation 3, sublimation rate from Equation 10, wind-driven unloading using Equation 11, and melt induced unloading from Equation 13 was assessed against observed canopy snow ablation from the weighed tree across 17 post-snowfall periods. These ablation periods had air temperatures ranging from -30.5°C to 6.9°C and wind speeds from calm to 5.3 m s⁻¹ (Table 3). The contribution of canopy snowmelt (and associated unloading), sublimation, and wind-driven unloading was used to classify individual events as either melt, sublimation, wind, or mixed (combination of many processes) dominated (Fig. 6). Melt dominated events had a fraction of over 0.85 of total ablation and had the least contribution from wind and sublimation (0 to 0.13). Sublimation and wind dominated events had minimal contribution of melt but due to the correlation of these two processes were difficult to isolate from one another.

The observed and simulated canopy snow load over each of the ablation events is shown in Fig. 7. When averaged over all events the updated routine resulted in a reduced mean bias of 0.04 mm hr⁻¹ compared to existing models which had a mean biases ranging from 0.06 to 0.12 mm hr⁻¹ when assessed with hourly weighed tree ablation and averaged across all events (Table 4). For the melt-dominated events, the two parameterizations that include an energy balance based routine track the observed decline in snow load over the melt process well in Fig. 7 with mean biases in hourly ablation of -0.03 mm hr⁻¹ and -0.06 mm hr⁻¹ for the new and Andreadis2009 routine respectively and a small range in mean biases across the differing melt events (Fig. 8). The air temperature (roesch2001) and ice-bulb temperature (Ellis2010) based routines have less consistency over these events (Fig. 8) resulting in mean biases of 0.28 to 0.41 mm hr⁻¹. The slight improvement for the updated routine compared to Andreadis2009 comes from the better representation of the increase in unloading for higher canopy snow loads (Equation 14) as observed for the 2022-06-14 event which had much higher snow load of 30 mm.

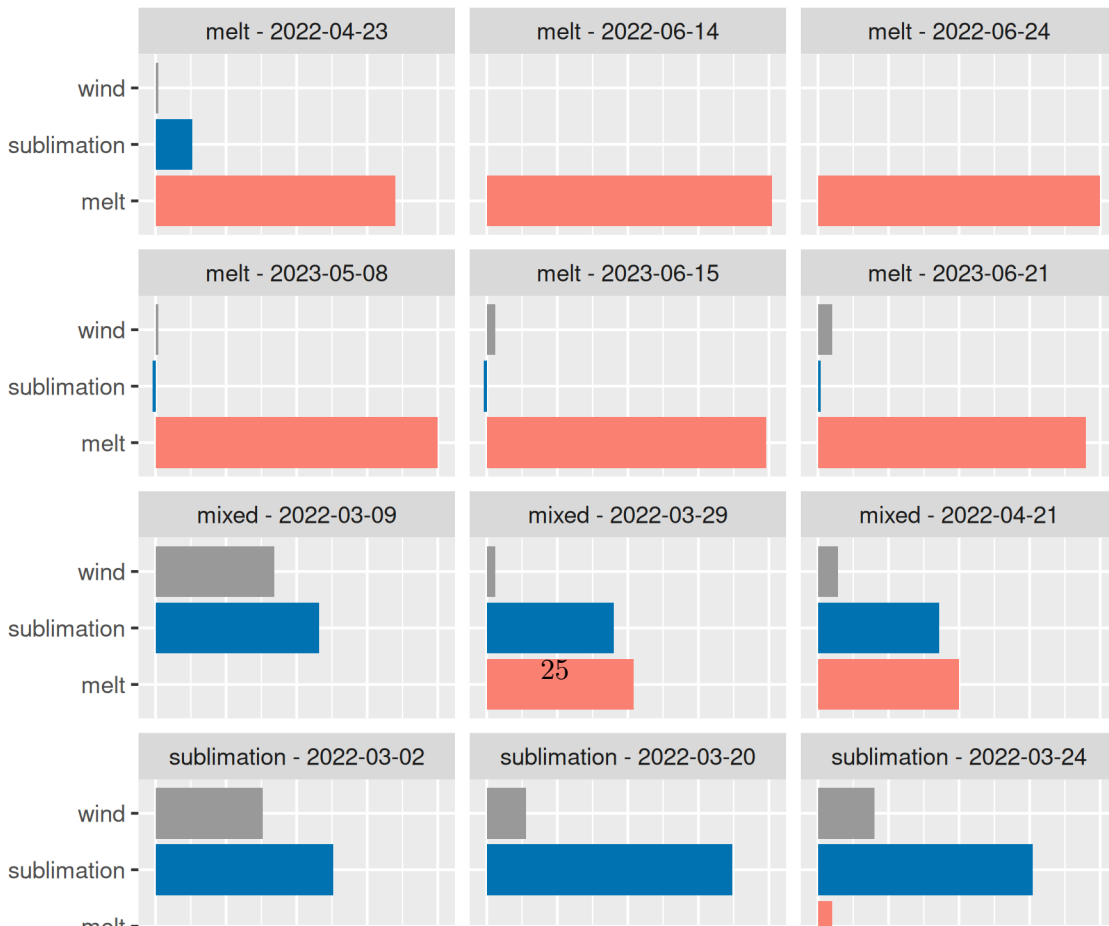
A small improvement in the mean bias over all events was observed for sublimation events in the updated routine, of -0.02 mm hr^{-1} compared to the other models which ranged from -0.04 to $NA \text{ mm hr}^{-1}$ (Table 4). The ellis2010 and andreadis2009 parameterizations resulted in a larger range in mean biases across the events (Fig. 8) particularly during clear-sky nights, which led to cooling of the canopy snow surface temperature and thus suppression of the canopy snow sublimation rate. This effect could be represented in the Essery et al. (2003) energy balance based routine but not in the Pomeroy et al. (1998) routine, which assumes that the canopy snow surface temperature remains in thermoequilibrium with the air temperature (Fig. 7). See event ‘2022-03-24’ in Fig. 7 for an example of this where the rate of sublimation slows at night and better matches the observation compared to the other models (and 2022-03-14 to a lesser extent). For relatively warm sublimation events, i.e., 2022-03-02 the ellis2010 and roesch2001 parameterizations over estimate ablation as they start to melt and unload snow from the canopy rapidly, while the energy balance method better captures the cooling effect of sublimation which suppresses the melt process (although the air temperature is above 0°C). Still some variability is observed with the energy balance based routines where the magnitude of ablation is over estimated for the 2023-03-14 event for the new routine, likely due to over estimation of wind induced unloading (on average), the timing of sublimation by the andreadis2009 routine is good here but it does not include wind unloading at all so misses the steep decline in canopy snow during specific wind periods the Ellis2010 routine over estimates total ablation here as well due to over estimation of sublimation at night due to night time cooling effects and inclusion of time induced unloading.

The wind-driven unloading events show the importance of representing this process, with models that simulate wind-induced unloading having lower mean bias of 0.21 mm hr^{-1} for the Roesch et al. (2001) linear model and 0.29 mm hr^{-1} in the updated model, compared to the mean bias of over 0.57 mm hr^{-1} for the two simulations that do not directly incorporate wind-induced unloading (Table 4). The roesch2001 parameterization over estimates the mean event unloading for two of the events, the updated routine is slightly more stable across the differing events, but still underestimates mean event for event 2023-02-24 which has peak wind speeds

of over 5 m s^{-1} and potentially some amount of wind transport process which is not directly accounted for. The wind induced unloading process resulted in the overall mean bias compared to the melt and sublimation dominated events, even compared to the wind unloading function developed at the same site (from the subcanopy lysimeters).

Table 3: Meteorology of the 17 select ablation events. Air temperature, relative humidity, and wind speed were measured at FT station. The process fractions show the fraction of canopy snow ablation for each process.

Start Date	Event Type	Air Temperature (°C)			Wind Speed (m/s)			Relative Humidity (%)			Process %
		Min	Mean	Max	Min	Mean	Max	Min	Mean	Max	
19105	melt	-1.8	2.0	5.3	0.4	0.8	1.2	35.8	60.2	82.8	0.8
19157	melt	0.1	3.1	6.9	0.1	0.8	1.7	66.6	90.6	99.8	1.0
19167	melt	0.8	3.4	5.7	0.2	0.6	1.1	82.5	89.7	97.8	1.0
19485	melt	0.9	2.1	4.4	0.4	0.7	1.0	91.1	96.7	98.6	1.0
19523	melt	0.5	3.0	6.8	0.7	1.1	1.6	76.7	93.3	99.4	1.0
19529	melt	-1.0	1.4	5.5	0.9	1.3	1.8	81.3	95.0	100.0	0.9
19080	mixed	-5.6	0.6	4.7	0.3	1.0	1.6	31.1	57.1	93.2	0.5
19103	mixed	-7.2	-0.4	3.4	0.5	1.0	1.9	47.8	65.9	95.2	0.5
19053	sublimation	-3.9	-2.1	0.9	0.0	0.9	2.1	59.4	88.0	97.6	0.0
19060	sublimation	-25.2	-15.7	-7.6	0.0	1.6	3.9	35.3	62.4	100.0	0.0
19071	sublimation	-8.1	-6.0	-3.9	0.4	1.4	3.5	44.4	63.4	89.7	0.0
19075	sublimation	-8.7	-2.7	3.8	0.1	1.1	3.6	29.3	55.0	99.6	0.0
19430	sublimation	-12.4	-6.6	3.0	0.4	1.2	2.3	22.7	59.4	89.3	0.0
19464	sublimation	-6.7	-4.6	-2.2	0.9	2.1	4.3	23.8	55.2	94.2	0.0
19327	wind	-21.7	-13.8	-3.1	0.5	1.7	4.5	41.0	83.6	100.0	0.0
19412	wind	-30.5	-21.3	-14.8	1.4	2.4	5.3	53.9	83.5	100.0	0.0
19414	wind	-12.8	-11.8	-10.3	0.8	1.4	2.0	70.6	82.7	95.3	0.0



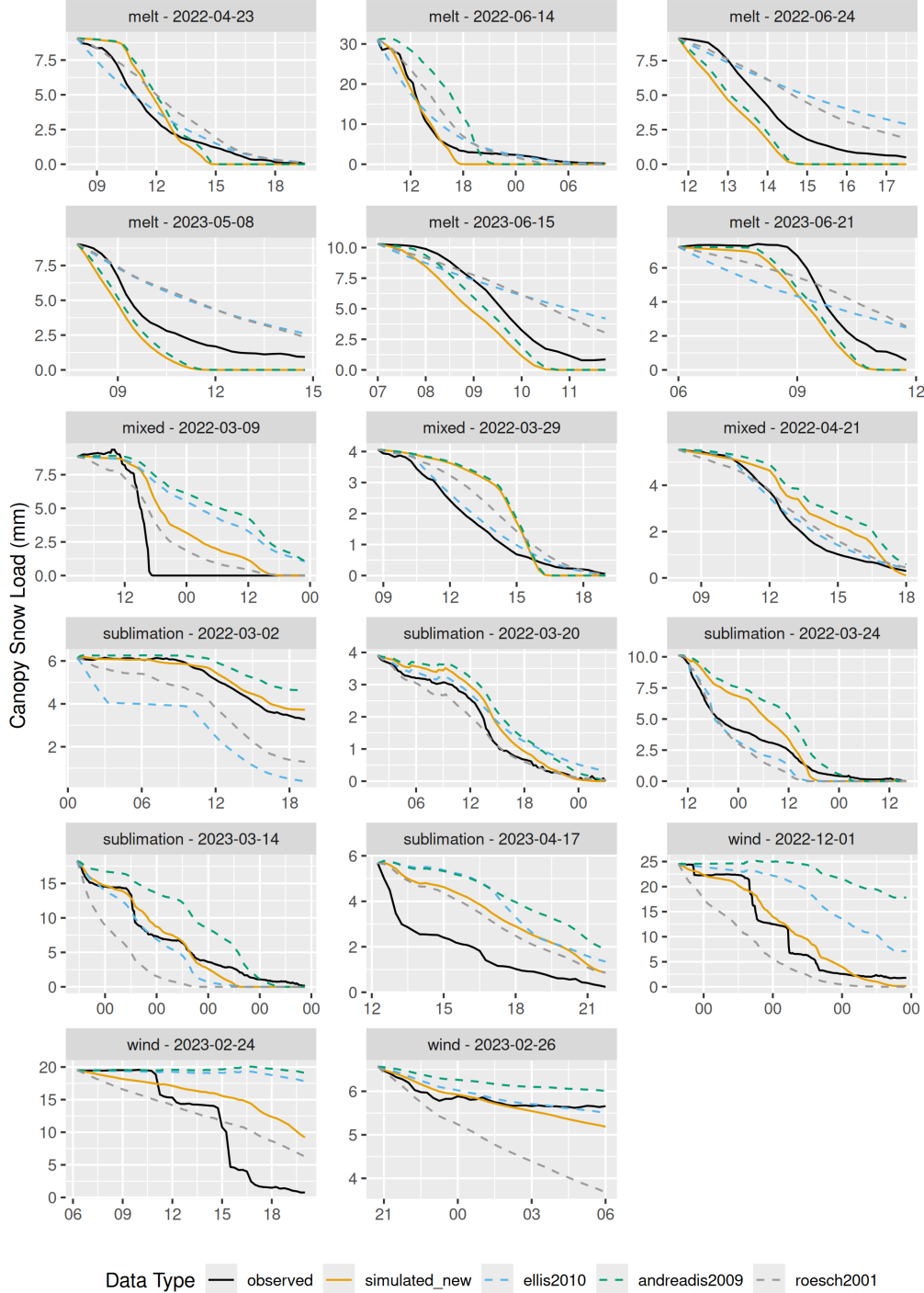


Figure 7: Canopy snow load time series for individual events measured by the weighed tree (Observed) and simulated using the various parameterisation sets.

Table 4: Model error statistics between hourly observed (weighed tree) and simulated (CRHM) canopy snow ablation. The Mean bias (MB) is the difference in the model and observed values, MAE is the mean of the absolute error, RMSE is the root mean squared error, NRMSE is the normalised RMSE, R is the pearson correlation coefficient, and R^2 is the pearson correlation coefficient squared. The ‘name’ column represents the parameterisation set used to simulate canopy snow ablation.

Model Name	Type	Event	RMS			
			Mean Bias (mm/hr)	MAE (mm/hr)	Error (mm/hr)	R^2
andreadis2009	melt		-0.06	0.67	0.91	0.57
simulated_new	melt		-0.03	0.67	0.84	0.63
roesch2001	melt		0.28	0.75	1.04	0.51
ellis2010	melt		0.41	0.79	1.14	0.40
roesch2001	mixed		0.15	0.35	0.47	0.52
simulated_new	mixed		0.17	0.46	0.63	0.21
ellis2010	mixed		0.23	0.32	0.46	0.73
andreadis2009	mixed		0.24	0.49	0.69	0.22
ellis2010	sublimation		-0.04	0.17	0.26	0.35
roesch2001	sublimation		-0.04	0.13	0.18	0.54
simulated_new	sublimation		-0.02	0.13	0.19	0.42
andreadis2009	sublimation		0.01	0.16	0.22	0.28
roesch2001	wind		0.21	0.70	1.06	0.40
simulated_new	wind		0.29	0.70	1.06	0.37
ellis2010	wind		0.57	0.70	1.18	0.41
andreadis2009	wind		0.67	0.71	1.22	0.47
simulated_new	all		0.04	0.32	0.67	0.47
roesch2001	all		0.06	0.34	0.70	0.40
ellis2010	all		0.12	0.33	0.78	0.26
andreadis2009	all		0.12	0.37	0.86	0.21

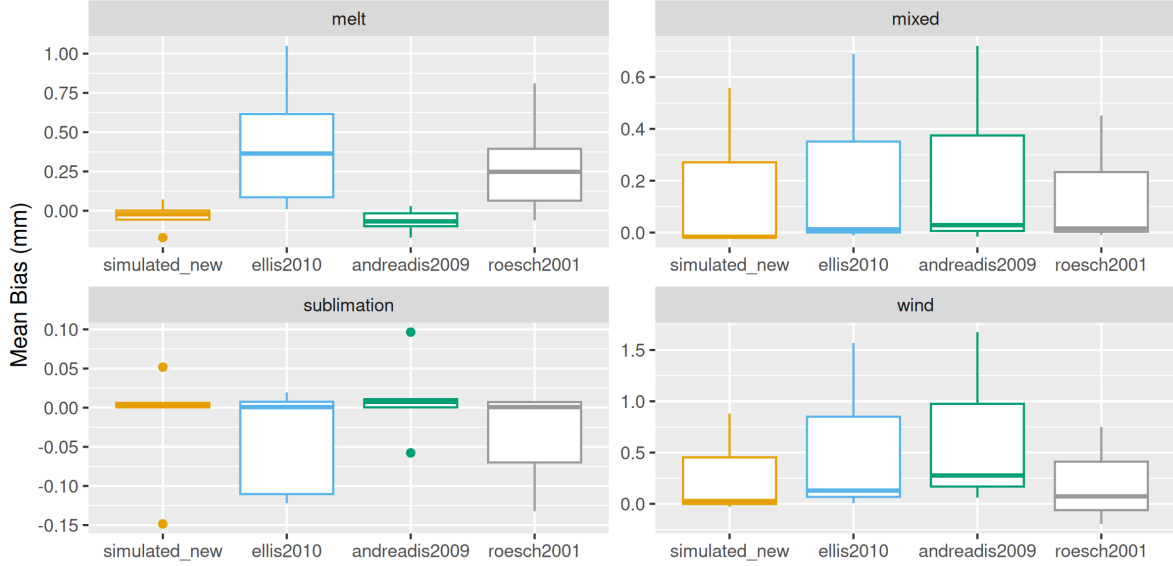


Figure 8: Boxplots illustrating the distribution of mean bias in hourly canopy snow ablation simulations across different parameterisation sets for each event type, evaluated using observations from the weighed tree.

7 Discussion

The inclusion of processes that ablate snow intercepted in the canopy is prevalent in many parameterisations for the initial loading of snow within the canopy. Many of these processes are related to the amount of time that snow resides in the canopy prior to the interception measurement was conducted in addition to wind and temperature induced unloading processes. After filtering out unloading due to temperature and wind the duration snow was intercepted in the canopy was found as a third important factor to consider. Unloading due to duration initially starts high while the snow is fresh and has low cohesion and adhesion and as the snow metamorphoses the adhesion and cohesion increases for the first 15 hours and the probability of unloading declines. After 15 hours the probability of unloading increases potentially due to increased sublimation and metamorphism of snow intercepted in the canopy which reduces its adhesion and cohesion.

A new unloading routine could be established based on these observations after filtering to remove temperature and wind induced unloading which show the probability of unloading after this filtering is high after initial loading of snow intercepted in the canopy, followed by a decline in probability until around 15 hours, and increases afterwards. This could be combined with the unloading rate which was observed to be high as the snow was initially loaded in the canopy and then declines steadily with increasing duration.

Based on the canopy snowmelt model, the Storck et al. (2002) ratio based melt based unloading parameterisation over estimates drip. It could also be that the parv snowmelt model is underestimating the canopy snow temperature.

Generally, model over estimates canopy snow wind induced unloading when wind speed < 1 m/s (see weighed tree events 2023-02-26, 2023-01-28). Under estimates when wind speed > 1 m/s (see events 2023-02-24).

Sometimes the overestimate of wind unloading for < 1 m/s is associated with higher canopy snow loads (see 2023-02-24 at the start, and 2023-03-14 at the start). But not necessarily for 2022-12-01 and 2023-03-25/26/28 which both either underestimate q_{unld}^{wind} or have good performance with high canopy snow loads.

Underestimates canopy snowmelt for colder/near 0 events (see 2023-03-25)

2023-03-26 not sure why ablation late on the 26th, as high humidity (~100%) and not too high wind speeds (~1m/s)

The wind dominated ablation events have much poorer performance, aside from 2022-12-01 which aligns well on average.

The sublimation or snowmelt dominated events, which are less influenced by wind have the best performance.

The wind model is slightly less sensitive, with lower unloading rates at the same wind speeds compared to the Roesch et al. (2001) relationships.

Not currently taking into account different density of unloaded snow, or over time as it melts in the canopy.

The melt unloading ratio increases with canopy snowmelt rate which as a result also increases as a function of canopy snowmelt. Air temperature is also indirectly included as canopy snowmelt is also a function of air temperature in this model. Air temperature could also have a negative impact on canopy snow unloading as a result of melt but this was not found in the observations presented here due to the larger effect of melt on unloading compared to the relationship with adhesion and cohesion and air temperature along.

Model does not account for wind redistribution of snow which may underestimate for some windy events or branch bending due to warming (directly) or warming of the canopy surface greater than the air temperature.

Unloading rate proportional to sublimation may also handle unloading/snowmelt not captured by current canopy snow algorithm which has canopy snow temperature equal to air temperature

Energy balance method relies on quality net radiation measurements which are not always certain while air temperature based methods may be more reliable.

The improved representation of the canopy snowmelt process is attributed to an improved representation of the energy to the canopy snowpack as described in Equation 3. This allows rate of canopy snowmelt to better reflect the available energy and also Equation 13 helps represent the associated increase in canopy snow unloading with snowmelt (Fig. 7). Another benefit of the energy balance method is it allows the canopy snow to cool during clear nights where the LW losses are greater than incoming LW from the atmosphere due to low atmospheric emissivity from lack of clouds which improved the simulation of the sublimation events see event 2022-03-24 in 7. Compared to the previous model which ablate at a higher rate due to increased sublimation driven by low humidities without considering the surface temperature cooling.

Improved representation of wind-induced unloading could be obtained by tracking the adhesion of snow to the canopy through melt/freeze or vapour deposition processes and cohesion due to equitemperature metamorphasm.

remaining gap on how much liquid water the canopy / canopy snow can hold.

much higher snow loads observed in Cebulski & Pomeroy (2025a) and thus the exposure coef in Pomeroy et al. (1998) was adjusted

despite not including the wind transport process, the new model performed well for windy events.

the higher variability of unloading during melt periods may have muted the wind induced unloading signal for these periods.

Essery et al. (2003) latent heat resistance as function of canopy fullness not included in Essery et al. (2025)

More canopy snow unloading with wind when snow is not melting (less cohesive and less dense)

the temperature of snowfall was observed as a rough indicator of the influence of temp on unloading. if snow fell cold branches were stiff and more horizontal, if fell warm then branches were more compressible theres a lag effect there that may have limited the influence of air temp on unloading in our observations

While there are advantages of treating initial interception and ablation processes separately, these parameterizations still need to be combined and tested together.

From JP: The shear stress makes better physical sense than wind speed for erosion or triggered of canopy snow by wind as it relates to the kinetic energy. It makes sense that this is for times when the intercepted snow is not melting and so is less cohesive and probably less dense.

Although only slight improvement was found for the incluin of the unloading to melt ratio as a function of canopy snow load. This would be expected to have a much more drastic

improvement in areas with very high snow loads over longer periods of time compared to those observed in this study.

8 Conclusions

- When considering all canopy snow ablation periods in our observations canopy snow load, wind speed, and canopy snowmelt were found to be statistically significant predictors, explaining 80% in the variability in canopy snow unloading.
- Shear stress, was found to be a stronger predictor of canopy snow unload ($R^2 = 0.66$) compared to wind speed ($R^2 = 0.52$) for non-melt periods.
- The observed associations of canopy snow unloading with wind speed and snowmelt were represented in a new canopy snow ablation routine. A linear function represents the increase in canopy snow unloading with mid canopy level shear stress which is also moderated by canopy snow load. Snow unloading during melt is represented as a ratio of the snow melt rate which depends on the canopy snow load. This routine accounts for cooling effects when snow evaporates from the canopy decreasing the rate of temperature induced unloading for increased wind speeds.
- Switching from temperature based canopy snow melt methods to an energy balance driven approach resulting in drastic improvements in representing canopy snow ablation
- Representing canopy snow sublimation using a robust energy balance approach is crucial for capturing snow accumulation in forests.
- The canopy snow exposure coef from existing studies was found to be too small at this site and needed to be increased substantially
- The proposed new model is more consistent across a wide range of temperatures and wind speeds.

9 Supporting Information

Table 5: Summary of multiple linear regression results evaluating all combinations of predictor variables for canopy snow unloading including: canopy load (L), wind speed (u), canopy snowmelt rate (q_{melt}), canopy snow sublimation rate (q_{subl}), and air temperature (T_a). Columns L to Ta show the coefficient estimate for each respective term, and the significance of each term is shown in brackets. Significance codes: * = $p < 0.05$; ns = not significant ($p > 0.05$). The models are ranked by their corresponding AIC value.

Model		Name	Intercept	L	u	q_{melt}	q_{subl}	τ	T_a	R^2	AIC
M1			-0.11	0.02 (*)	0.08 (*)	0.40 (*)	—	—	—	0.79	-12.8
				(ns)							
M2			-0.06	0.02	—	0.41 (*)	—	—	—	0.76	10.7
				(ns)	(ns)						
M3			0.10	0.01	—	0.35 (*)	—	—	0.00	0.72	6.7
				(ns)	(ns)				(ns)		
M4			-0.08	0.04 (*)	—	0.39 (*)	—	0.75	—	0.71	5.5
				(ns)					(*)		
M5			-0.12	0.02 (*)	0.08 (ns)	0.40 (*)	—	0.04	—	0.71	-7.6
				(ns)					(ns)		
M6			0.17 (*)	0.01	—	0.31 (*)	—	—	0.00	0.57	-4.9
				(ns)					(ns)		
M7			0.13	0.02 (*)	—	0.32 (*)	-0.22	—	—	0.54	10.0
				(ns)			(ns)				
M8			0.10	0.01	—	0.32 (*)	—	—	—	0.53	23.6
				(ns)	(ns)						
M9			0.02	0.02 (*)	—	0.37 (*)	—	0.77	-0.00	0.53	2.2
				(ns)					(*)	(ns)	
M10			-0.06	0.02 (*)	0.08 (*)	0.38 (*)	—	—	0.00	0.52	-4.4
				(ns)					(ns)		

Table 5: Summary of multiple linear regression results evaluating all combinations of predictor variables for canopy snow unloading including: canopy load (L), wind speed (u), canopy snowmelt rate (q_{melt}), canopy snow sublimation rate (q_{subl}), and air temperature (T_a). Columns L to Ta show the coefficient estimate for each respective term, and the significance of each term is shown in brackets. Significance codes: * = $p < 0.05$; ns = not significant ($p > 0.05$). The models are ranked by their corresponding AIC value.

Model									
Name	Intercept	L	u	q_{melt}	q_{subl}	τ	T_a	R^2	AIC
M11	-0.00	0.02 (*)	0.05 (*)	0.35 (*)	—	—	—	0.49	-5.8
		(ns)							
M12	0.28 (*)	0.01	—	—	—	—	0.01	0.45	-25.0
		(ns)							
M13	-0.02	0.03 (*)	—	0.37 (*)	0.06 (ns)	0.97	—	0.45	-9.7
		(ns)							
M14	-0.06	0.02 (*)	0.08 (ns)	0.38 (*)	—	0.18	0.00	0.45	5.5
		(ns)							
M15	-0.03	0.02 (*)	0.07 (*)	—	—	—	—	0.43	-34.8
		(ns)							
M16	-0.01	0.02 (*)	—	0.35 (*)	-0.25	1.15	—	0.41	-35.2
		(ns)							
M17	0.06	0.01 (*)	—	0.34 (*)	—	0.77	0.00	0.41	-2.9
		(ns)							
M18	-0.01	0.01	—	—	—	—	—	0.40	-11.9
		(ns)							
M19	0.11	0.01	—	0.33 (*)	0.15 (ns)	—	-0.00	0.39	6.4
		(ns)							
M20	0.05	0.01 (*)	0.06 (*)	0.34 (*)	—	—	0.00	0.39	-10.5
		(ns)							

Table 5: Summary of multiple linear regression results evaluating all combinations of predictor variables for canopy snow unloading including: canopy load (L), wind speed (u), canopy snowmelt rate (q_{melt}), canopy snow sublimation rate (q_{subl}), and air temperature (T_a). Columns L to Ta show the coefficient estimate for each respective term, and the significance of each term is shown in brackets. Significance codes: * = $p < 0.05$; ns = not significant ($p > 0.05$). The models are ranked by their corresponding AIC value.

Model									
Name	Intercept	L	u	q_{melt}	q_{subl}	τ	T_a	R^2	AIC
M21	-0.02	0.03 (*)	—	0.35 (*)	—	0.67	—	0.38	55.7
		(ns)					(*)		
M22	0.02	0.02 (*)	-0.02	0.35 (*)	—	0.84	—	0.38	42.1
		(ns)		(ns)			(ns)		
M23	0.00	0.02 (*)	—	0.36 (*)	0.08 (ns)	1.10	0.00	0.38	-10.0
		(ns)					(*)	(ns)	
M24	-0.00	0.02 (*)	0.05 (*)	0.36 (*)	0.13 (ns)	—	—	0.37	-2.0
		(ns)							
M25	0.05	0.02 (*)	-0.05	0.35 (*)	0.05 (ns)	1.46	—	0.36	0.2
		(ns)		(ns)			(*)		
M26	0.09	0.01	0.02 (ns)	0.34 (*)	—	0.46	0.00	0.36	1.9
		(ns)	(ns)				(ns)	(ns)	
M27	0.08	0.02 (*)	—	0.32 (*)	-0.20	0.95	0.00	0.35	-24.2
		(ns)			(ns)		(*)	(ns)	
M28	0.15 (*)	0.01 (*)	-0.09	0.31 (*)	-0.13	1.68	—	0.31	-6.9
			(ns)		(ns)		(*)		
M29	-0.00	0.03 (*)	—	—	—	0.59	—	0.30	-5.0
		(ns)					(*)		
M30	0.15 (*)	0.02 (*)	—	0.31 (*)	0.06 (ns)	—	—	0.30	43.7
M31	0.03	0.01 (*)	0.06 (*)	0.35 (*)	-0.03	—	0.00	0.28	28.0
		(ns)			(ns)			(ns)	

Table 5: Summary of multiple linear regression results evaluating all combinations of predictor variables for canopy snow unloading including: canopy load (L), wind speed (u), canopy snowmelt rate (q_{melt}), canopy snow sublimation rate (q_{subl}), and air temperature (T_a). Columns L to Ta show the coefficient estimate for each respective term, and the significance of each term is shown in brackets. Significance codes: * = $p < 0.05$; ns = not significant ($p > 0.05$). The models are ranked by their corresponding AIC value.

Model									
Name	Intercept	L	u	q_{melt}	q_{subl}	τ	T_a	R^2	AIC
M32	0.03 (ns)	0.02 (*) (ns)	0.04 (ns)	0.35 (*)	-0.07 (ns)	0.63 (ns)	0.00 (ns)	0.27	38.5
M33	-0.05 (ns)	0.02 (*) (ns)	0.06 (ns)	—	—	0.09	— (ns)	0.25	-18.8
M34	-0.02 (ns)	0.02 (*) (ns)	0.07 (*)	0.34 (*)	-0.22 (ns)	—	—	0.24	70.7
M35	0.11 (ns)	0.01 (*) (ns)	—	0.32 (*)	0.24 (ns) (ns)	—	-0.00 (ns)	0.23	59.2
M36	0.20 (*) (ns)	0.01 (ns)	0.01 (ns)	0.28 (*)	-0.11 (ns)	—	0.01 (ns)	0.21	50.2
M37	0.21 (*) (ns)	0.01 (ns)	0.00 (ns)	0.28 (*)	-0.14 (ns)	0.31 (ns)	0.01 (ns)	0.19	65.6
M38	-0.08 (ns)	0.03 (*) (ns)	—	—	—	0.68 (*)	—	0.16	35.7
M39	-0.03 (ns)	0.02 (*) (ns)	0.04 (*)	—	—	—	—	0.14	-41.7
M40	0.07 (ns)	0.01 (*) (ns)	0.06 (*)	—	—	—	0.01 (ns)	0.11	2.4
M41	0.30 (*) (ns)	0.01 (ns)	—	—	—	—	0.01 (*)	0.11	10.5

Table 5: Summary of multiple linear regression results evaluating all combinations of predictor variables for canopy snow unloading including: canopy load (L), wind speed (u), canopy snowmelt rate (q_{melt}), canopy snow sublimation rate (q_{subl}), and air temperature (T_a). Columns L to Ta show the coefficient estimate for each respective term, and the significance of each term is shown in brackets. Significance codes: * = $p < 0.05$; ns = not significant ($p > 0.05$). The models are ranked by their corresponding AIC value.

Model										
Name	Intercept	L	u	q_{melt}	q_{subl}	τ	T_a	R^2	AIC	
M42	0.01	0.02 (*)	-0.02	—	—	0.85	—	0.11	20.3	
	(ns)		(ns)			(ns)				
M43	0.08	0.01 (*)	—	—	—	0.65	0.00	0.10	-9.2	
	(ns)					(*)	(ns)			
M44	0.05	0.01 (*)	0.05 (ns)	—	—	0.21	0.00	0.07	13.6	
	(ns)					(ns)	(ns)			
M45	0.30 (*)	0.01	-0.17 (*)	—	-0.27	2.27	—	0.07	37.8	
	(ns)				(ns)	(*)				
M46	0.21 (*)	0.01 (*)	—	—	-0.36	0.68	0.01	0.07	31.4	
					(ns)	(*)	(*)			
M47	0.35 (*)	0.00	-0.02	—	-0.27	—	0.01	0.06	83.6	
	(ns)	(ns)			(ns)		(*)			
M48	0.45 (*)	0.00	—	—	-0.72	—	—	0.05	33.7	
	(ns)				(ns)					
M49	0.18 (*)	0.02 (*)	—	—	-0.08	0.72	0.01	0.05	45.6	
					(ns)	(*)	(*)			
M50	0.08	0.01 (*)	—	—	-0.40	0.77	—	0.05	33.3	
	(ns)				(ns)	(*)				
M51	0.16 (*)	0.01 (*)	—	—	—	0.54	0.01	0.05	24.4	
						(*)	(ns)			

Table 5: Summary of multiple linear regression results evaluating all combinations of predictor variables for canopy snow unloading including: canopy load (L), wind speed (u), canopy snowmelt rate (q_{melt}), canopy snow sublimation rate (q_{subl}), and air temperature (T_a). Columns L to Ta show the coefficient estimate for each respective term, and the significance of each term is shown in brackets. Significance codes: * = $p < 0.05$; ns = not significant ($p > 0.05$). The models are ranked by their corresponding AIC value.

Model										
Name	Intercept	L	u	q_{melt}	q_{subl}	τ	T_a	R^2	AIC	
M52	0.29 (*)	0.01 (ns)	-0.15 (*)	—	0.02 (ns)	1.99 (*)	—	0.04	41.6	
M53	0.17 (*)	0.01 (ns)	0.04 (*)	—	—	—	0.01 (ns)	0.04	25.5	
M54	0.36 (*)	0.00 (ns)	-0.04 (ns)	—	-0.31 (ns)	0.51 (ns)	0.01 (*)	0.04	95.1	
M55	0.11	0.02 (*) (ns)	0.03 (ns)	—	-0.38 (ns)	—	—	0.03	105.6	
M56	0.26 (*)	0.01 (*) (ns)	-0.03 (ns)	—	-0.21 (ns)	1.01 (ns)	0.01 (*)	0.03	84.2	
M57	0.22 (*)	0.01 (ns)	-0.02 (ns)	—	—	0.61 (ns)	0.01 (ns)	0.03	36.4	
M58	0.17 (*)	0.02 (*)	—	—	-0.08 (ns)	0.38 (ns)	—	0.02	39.3	
M59	0.24 (*)	0.01 (ns)	0.02 (ns)	—	-0.16 (ns)	—	0.01 (*)	0.02	76.0	
M60	0.33 (*)	0.01 (ns)	—	—	-0.17 (ns)	—	0.01 (ns)	0.01	44.0	
M61	0.23 (*)	0.01 (*)	—	—	0.03 (ns)	—	0.01 (ns)	0.01	94.3	

Table 5: Summary of multiple linear regression results evaluating all combinations of predictor variables for canopy snow unloading including: canopy load (L), wind speed (u), canopy snowmelt rate (q_{melt}), canopy snow sublimation rate (q_{subl}), and air temperature (T_a). Columns L to Ta show the coefficient estimate for each respective term, and the significance of each term is shown in brackets. Significance codes: * = $p < 0.05$; ns = not significant ($p > 0.05$). The models are ranked by their corresponding AIC value.

Model		Name	Intercept	L	u	q_{melt}	q_{subl}	τ	T_a	R^2	AIC
M62			0.24 (*)	0.01	—	—	-0.18	—	—	-0.01	75.2
					(ns)		(ns)				
M63			0.22 (*)	0.00	-0.01	—	0.07 (ns)	—	—	-0.02	39.8
					(ns)	(ns)					

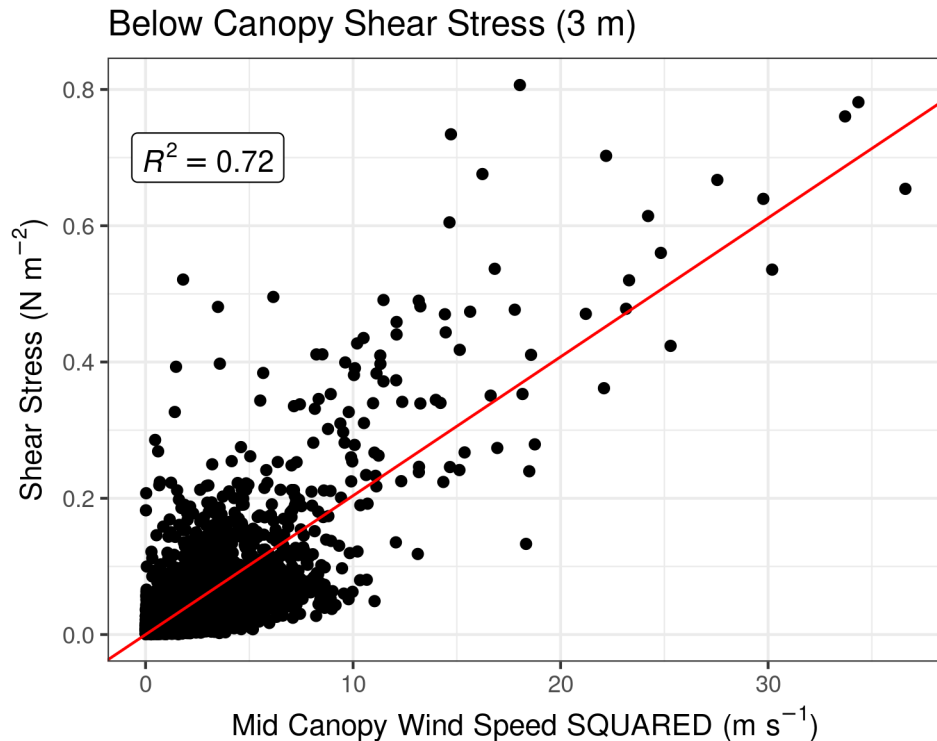
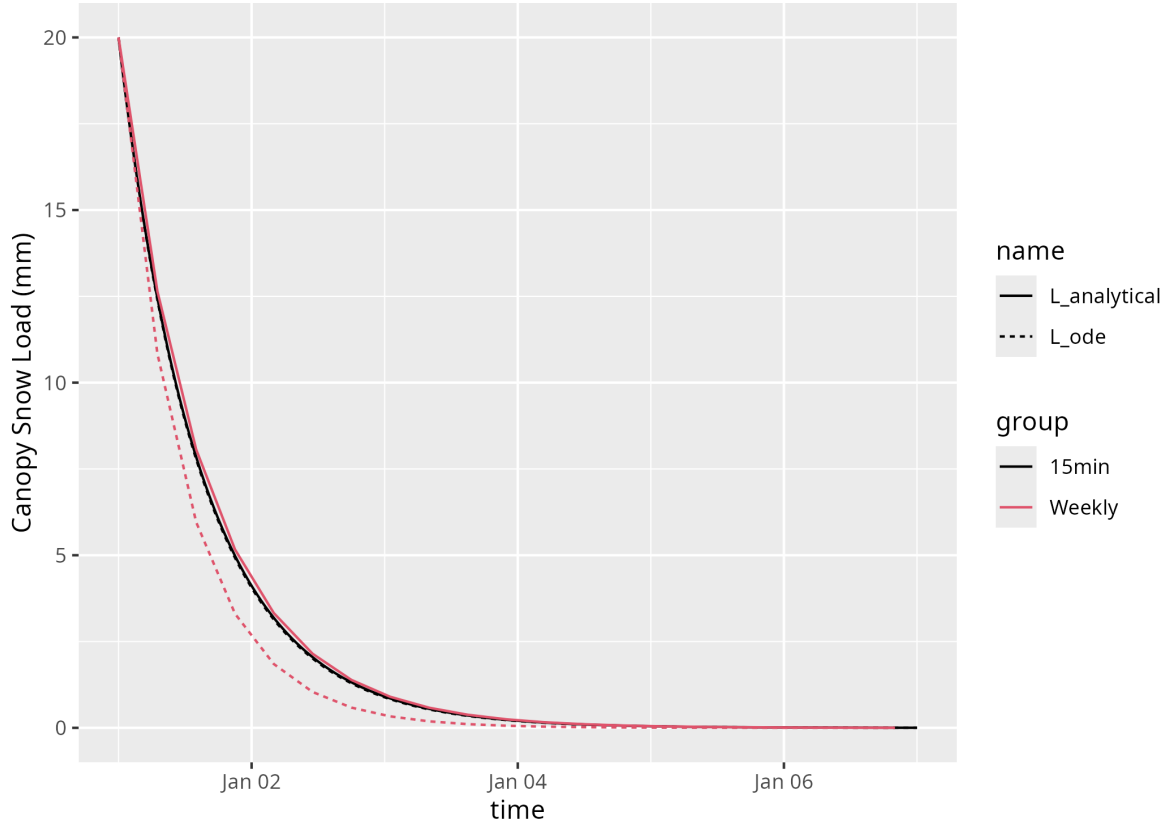


Figure 9: Wind speed versus shear stress relationship.



References

- Allan, R., Pereira, L., Raes, D., & Smith, M. (1998). *Crop evapotranspiration Guidelines for computing crop water requirements*. Food and Agriculture Organization of the United Nations.
- Andreadis, K. M., Storck, P., & Lettenmaier, D. P. (2009). Modeling snow accumulation and ablation processes in forested environments. *Water Resources Research*, 45(5), 1–33. <https://doi.org/10.1029/2008WR007042>
- Cebulski, A. C., & Pomeroy, J. W. (2025a). Snow Interception Relationships With Meteorology and Canopy Density. *Hydrological Processes*, 39(4), e70135. <https://doi.org/10.1002/hyp.70135>
- Cebulski, A. C., & Pomeroy, J. W. (2025b). Theoretical Underpinnings of Snow Interception and Canopy Snow Ablation Parameterisations. *WIREs Water*, 12, e70010. <https://doi.org/10.1002/wat2.70010>

g/10.1002/wat2.70010

- Conway, J. P., Pomeroy, J. W., Helgason, W. D., & Kinar, N. J. (2018). Challenges in modeling turbulent heat fluxes to snowpacks in forest clearings. *Journal of Hydrometeorology*, 19(10), 1599–1616. <https://doi.org/10.1175/JHM-D-18-0050.1>
- Ellis, C. R., Pomeroy, J. W., Brown, T., & MacDonald, J. (2010). Simulation of snow accumulation and melt in needleleaf forest environments. *Hydrology and Earth System Sciences*, 14(6), 925–940. <https://doi.org/10.5194/hess-14-925-2010>
- Essery, R., Mazzotti, G., Barr, S., Jonas, T., Quaife, T., & Rutter, N. (2025). A Flexible Snow Model (FSM 2.1.0) including a forest canopy. *EGUphere*, 1–37. <https://doi.org/10.5194/egusphere-2024-2546>
- Essery, R., Pomeroy, J. W., Parviainen, J., & Storck, P. (2003). Sublimation of snow from coniferous forests in a climate model. *Journal of Climate*, 16(11), 1855–1864. [https://doi.org/10.1175/1520-0442\(2003\)016%3C1855:SOSFCF%3E2.0.CO;2](https://doi.org/10.1175/1520-0442(2003)016%3C1855:SOSFCF%3E2.0.CO;2)
- Floyd, W. C. (2012). *Snowmelt energy flux recovery during rain-on-snow in regenerating forests* (p. 180) [PhD thesis, University of British Columbia]. <https://doi.org/https://dx.doi.org/10.14288/1.0073024>
- Hedstrom, N. R., & Pomeroy, J. W. (1998). Measurements and modelling of snow interception in the boreal forest. *Hydrological Processes*, 12(10-11), 1611–1625. [https://doi.org/10.1002/\(SICI\)1099-1085\(199808/09\)12:10/11%3C1611::AID-HYP684%3E3.0.CO;2-4](https://doi.org/10.1002/(SICI)1099-1085(199808/09)12:10/11%3C1611::AID-HYP684%3E3.0.CO;2-4)
- Helgason, W., & Pomeroy, J. W. (2012a). Characteristics of the near-surface boundary layer within a mountain valley during winter. *Journal of Applied Meteorology and Climatology*, 51(3), 583–597. <https://doi.org/10.1175/JAMC-D-11-058.1>
- Helgason, W., & Pomeroy, J. W. (2012b). Problems closing the energy balance over a homogeneous snow cover during midwinter. *Journal of Hydrometeorology*, 13(2), 557–572. <https://doi.org/10.1175/JHM-D-11-0135.1>
- Kesselring, J., Morsdorf, F., Kükenbrink, D., Gastellu-Etchegorry, J.-P., & Damm, A. (2024). Diversity of 3D APAR and LAI dynamics in broadleaf and coniferous forests: Implications for the interpretation of remote sensing-based products. *Remote Sensing of Environment*, 306, 114116. <https://doi.org/10.1016/j.rse.2024.114116>

- Pomeroy, J. W., Gray, D. M., Brown, T., Hedstrom, N. R., Quinton, W. L., Granger, R. J., & Carey, S. K. (2007). The cold regions hydrological model: A platform for basing process representation and model structure on physical evidence. *Hydrological Processes*, 21(19), 2650–2667. <https://doi.org/10.1002/hyp.6787>
- Pomeroy, J. W., Marks, D., Link, T., Ellis, C. R., Hardy, J., Rowlands, A., & Granger, R. (2009). The impact of coniferous forest temperature on incoming longwave radiation to melting snow. *Hydrological Processes*, 23, 2513–2525. <https://doi.org/10.1002/hyp.7325>
- Pomeroy, J. W., Parviainen, J., Hedstrom, N., & Gray, D. M. (1998). Coupled modelling of forest snow interception and sublimation. *Hydrological Processes*, 12(15), 2317–2337. [https://doi.org/10.1002/\(SICI\)1099-1085\(199812\)12:15%3C2317::AID-HYP799%3E3.0.CO;2-X](https://doi.org/10.1002/(SICI)1099-1085(199812)12:15%3C2317::AID-HYP799%3E3.0.CO;2-X)
- Pomeroy, J. W., & Schmidt, R. A. (1993). The use of fractal geometry in modelling intercepted snow accumulation and sublimation. *Eastern Snow Conference*, 50, 231–239.
- Roesch, A., Wild, M., Gilgen, H., & Ohmura, A. (2001). A new snow cover fraction parameterization for the ECHAM4 GCM. *Climate Dynamics*, 17(12), 933–946. <https://doi.org/10.1007/s003820100153>
- Sicart, J. E., Pomeroy, J. W., Essery, R. L. H., & Bewley, D. (2006). Incoming longwave radiation to melting snow: Observations, sensitivity and estimation in Northern environments. *Hydrological Processes*, 20(17), 3697–3708.
- Storck, P., Lettenmaier, D. P., & Bolton, S. M. (2002). Measurement of snow interception and canopy effects on snow accumulation and melt in a mountainous maritime climate, Oregon, United States. *Water Resources Research*, 38(11), 1–16. <https://doi.org/10.1029/2002wr001281>
- Weiskittel, A. R., Kershaw, J. A., Hofmeyer, P. V., & Seymour, R. S. (2009). Species differences in total and vertical distribution of branch- and tree-level leaf area for the five primary conifer species in Maine, USA. *Forest Ecology and Management*, 258(7), 1695–1703. <https://doi.org/10.1016/j.foreco.2009.07.035>